REPORT DOCUMENTATION PAGE

Form Approved
OMB No. 0704-0188

1. REPORT DATE *(DD-MM-YYYY)* 13-04-2009	**2. REPORT TYPE** Journal Article	**3. DATES COVERED** *(From - To)*

4. TITLE AND SUBTITLE

Photothermal Deoxygenation of Graphene Oxide to Graphitic Carbon for Distributed Ignition and Patterning Applications (Preprint)

5a. CONTRACT NUMBER

5b. GRANT NUMBER

5c. PROGRAM ELEMENT NUMBER

6. AUTHOR(S)

Scott Gilje & Jabarri Farrar (Northrop Grumman); Sergey Dubin & Richard B. Kaner (UCLA); Alireza Badakshan (Sverdrup); S.A. Danczyk (AFRL/RZSA)

5d. PROJECT NUMBER

5f. WORK UNIT NUMBER
43470876

7. PERFORMING ORGANIZATION NAME(S) AND ADDRESS(ES)

Air Force Research Laboratory (AFMC)
AFRL/RZSA
10 E. Saturn Blvd.
Edwards AFB CA 93524-7680

8. PERFORMING ORGANIZATION REPORT NUMBER

AFRL-RZ-ED-JA-2009-152

9. SPONSORING / MONITORING AGENCY NAME(S) AND ADDRESS(ES)

Air Force Research Laboratory (AFMC)
AFRL/RZS
5 Pollux Drive
Edwards AFB CA 93524-7048

10. SPONSOR/MONITOR'S ACRONYM(S)

11. SPONSOR/MONITOR'S NUMBER(S)
AFRL-RZ-ED-JA-2009-152

12. DISTRIBUTION / AVAILABILITY STATEMENT

Approved for public release; distribution unlimited (PA #09227).

13. SUPPLEMENTARY NOTES
For publication in Nano Letters and/or the Journal of Advanced Materials.

14. ABSTRACT

In recent years, several researchers have reported on an enhanced photothermal effect exhibited when nanoscale materials such as carbon nanotubes, polyaniline nanofibers or Si nanowires were irradiated using a photographic flash. **[1-3]**. In these studies, the high surface to volume ratio of the nanomaterials being flashed, coupled with the inability of the small structures to efficiently dissipate the absorbed energy, led to a rapid increase in temperature and subsequent ignition/welding of the materials. Although heating materials through the use of light energy is not a new phenomenon, achieving such a rapid and dramatic temperature change using only millisecond pulses of light demonstrates a tangible and technologically significant capability, unique to nanoscale materials. **[4]** We have been able to achieve an enhanced photothermally activated reaction by exposing nanostructured graphene oxide (GO) porous networks, to a photographic flash. The exposure results in a pronounced photoacoustic effect along with a rapid temperature increase, which initiates a secondary deoxygenation reaction to yield graphitic carbon and CO_2. A photo-initiated reaction could be used to achieve multiple ignition nucleation sites simultaneously. This type of "distributed ignition" has applications in liquid fuel rocket engines and in high efficiency homogenous charge compression ignition (HCCI) engines, where ignition control is of paramount importance.

15. SUBJECT TERMS

16. SECURITY CLASSIFICATION OF:			**17. LIMITATION OF ABSTRACT**	**18. NUMBER OF PAGES**	**19a. NAME OF RESPONSIBLE PERSON** Dr. S.A. Danczyk
a. REPORT **Unclassified**	**b. ABSTRACT** **Unclassified**	**c. THIS PAGE** **Unclassified**	SAR	15	**19b. TELEPHONE NUMBER** *(include area code)* N/A

Photothermal Deoxygenation of Graphene Oxide to Graphitic Carbon for Distributed Ignition and Patterning Applications

(PREPRINT)

Scott Gilje[1], Sergey Dubin[2], Alireza Badakshan[3], Jabarri Farar[1], S. A. Danczyk[3], Richard B Kaner[2].

1 - Northrop Grumman Corporation
2 - Department of Chemistry and Biochemistry, University of California Los Angeles, Los Angeles, California, 90095
3 - AeroPhysics Branch, Combustion Devices Group,
Air Force Research Laboratory; Edwards AFB, California

Abstract

In recent years, several researchers have reported on an enhanced photothermal effect exhibited when nanoscale materials such as carbon nanotubes, polyaniline nanofibers or Si nanowires were irradiated using a photographic flash. **[1-3]**. In these studies, the high surface to volume ratio of the nanomaterials being flashed, coupled with the inability of the small structures to efficiently dissipate the absorbed energy, led to a rapid increase in temperature and subsequent ignition/welding of the materials. Although heating materials through the use of light energy is not a new phenomenon, achieving such a rapid and dramatic temperature change using only millisecond pulses of light demonstrates a tangible and technologically significant capability, unique to nanoscale materials. **[4]** We have been able to achieve an enhanced photothermally activated reaction by exposing nanostructured graphene oxide (GO) porous networks, to a photographic flash. The exposure results in a pronounced photoacoustic effect along with a rapid temperature increase, which initiates a secondary deoxygenation reaction to yield graphitic carbon and CO_2. A photo-initiated reaction could be used to achieve multiple ignition nucleation sites simultaneously. This type of "distributed ignition" has applications in liquid fuel rocket engines and in high efficiency homogenous charge compression ignition (HCCI) engines, where ignition control is of paramount importance. We also demonstrate how thin films of GO can be flashed and even patterned using a mask to control exposure. This holds potential for future graphene and GO-based electronics.

Intro

Graphene oxide (GO) is a deeply colored, water dispersible, oxidized form of graphene obtained through the treatment of graphite powder with powerful oxidizing agents. Although its synthesis has existed in the literature for over 150 years, only recently have scientists had access to the tools necessary to properly analyze its individual atomically thin platelet structure.**[5]** This has rekindled interest in GO and has led to a number of discoveries in recent years including: the stacking of GO platelets to form paper-like materials of high modulus and strength **[6,7]** Of somewhat greater interest to some is the reduction/deoxygenation of GO through the use of chemical reducing agents such as hydrazine to yield a conducting form of graphene-like carbon.**[8-**

10]. This has led some to speculate that GO could find use as precursor material in a bulk route to dispersible graphene sheets.**[11-13]** Already, a number of groups have succeeded in creating conducting polymer composites, transparent conducting films, and simple electronic devices based on reduced GO. **[14-26]** In addition to the chemical reduction of GO, Aksay et al. have reported the thermal deoxygenation of GO to create functionalized graphene sheets (FGS) upon rapid heating to 1100 °C under inert atmosphere.**[27, 28]** These organic solvent dispersible FGS sheets have enabled the creation FGS/polymer composites directly, without the use of surfactants. **[29]** Thermal deoxygenation of GO to form graphitic carbon dates back to the 1960's when Sholz and Boehm first reported on the ignition and deflagration of GOs prepared by different methods. **[30]** With CO_2 being the thermodynamically most stable oxide of carbon, the metastable GO decomposition upon rapid heating to temperatures ~200 °C initiating the exothermic release of CO_2 and H_2O with CO as a minor product. **[31]**

Networks of nanoscopic, light absorbing materials have successfully demonstrated radiant energy confinement upon exposure to a photographic flash in the past resulting in the welding together of polyaniline fibers and ignition of carbon nanotubes (CNTs) and Si nanowires.**[1-3]** Ajayan explained this phenomenon stating, that the absorbance of light coupled with the inefficient dissipation resulted in temperatures in excess of 1500 °C. Due to the dramatic temperatures that can be achieved using millisecond pulse of light, CNTs have been considered in the past as additives to rocket fuels where they could be used to attain distributed ignition of the fuel, providing better control and stability while lowering weight.**[32-34]** Attempts aimed at using CNTs for ignition applications however have failed, since the combustion of CNTs requires outside oxygen to support combustion of the iron nanoparticle catalyst used to grown CNTs; the CNTs themselves – like C_{60} and carbon soot - play little role in the ignition process. **[35-37]** Uniformly dispersing CNTs into liquid fuels remain an issue as well. We have found that the photothermally initiated deflagration of GO can take place with no surrounding oxygen. GO readily disperses in alcohols, and with some chemical modification could disperse in other fuels as well. The current interest in GO as a nanoscale platelet material coupled with the initiation of GO deflagration to yield a graphitic form of carbon enticed us to investigate this photothermally driven process further.

Results:

We create random porous networks of GO platelets by freeze-drying GO dispersions at a variety of concentrations. This porous structure results from the drawing off of water without causing collapse of the solid matrix of GO platelets due to capillary action, as would happen with conventional evaporation. Creating dry, low-density networks of nanoscale GO platelets serves two purposes: first the surface to volume ratio of the platelets is increased providing maximum surface area for energy absorption. Second, thermally conductive pathways through which absorbed energy could diffuse are reduced. GO foam networks enable greater energy absorption and confinement can be achieved; as a result, more rapid and dramatic temperature increases can be achieved. It was found that using freeze-drying, porous GO foams could be made to densities of nominally 5 mg/cm^3 before the structures would collapse under their own weight. **Figure**

1a is a photograph of a light-brown GO foam sample prepared by freeze drying a 15 mg/ml dispersion to achieve a density of 15 mg/cm^3. **Figure 1b** shows an SEM micrograph of the same sample magnified 1000x. In the SEM image, the GO platelets appear as crumpled sheets ranging in size from 500 nm -20 μm in diameter, that assemble to form a porous 3-dimensional network. Trace amounts of water adhered to the surface of the GO sheets most likely hold the sheets together giving the foams some rigidity.

Upon exposure to a photographic flash, the GO foam emits a popping sound most likely attributed to a photoacoustic effect. **[38]** A color change from light brown to dark black can be witnessed immediately after flashing indicating conversion to deoxygenated graphitic carbon (DGC). A photograph of flashed GO foam appears in **Figure 1c.** The light brown spots around the periphery of the sample indicate unreacted regions at the edges of the sample as a result cooling and expansion of the foam as the reaction front propagated. **Figure 1d**, indicate an expanded structure much like that of exfoliated graphite, or more recently thermally reduced GO, termed functionalized graphene sheets (FGS). **[27, 28]** The inset picture of **Figure 1d** shows the flashed GO foam at 100,000x magnification. At this magnification, we can see the expanded nature of the flashed converted graphitic platelets. Using the scale bar as a gauge, we measured the thickness of the thinnest expanded sheets to range from 10-20 nm.

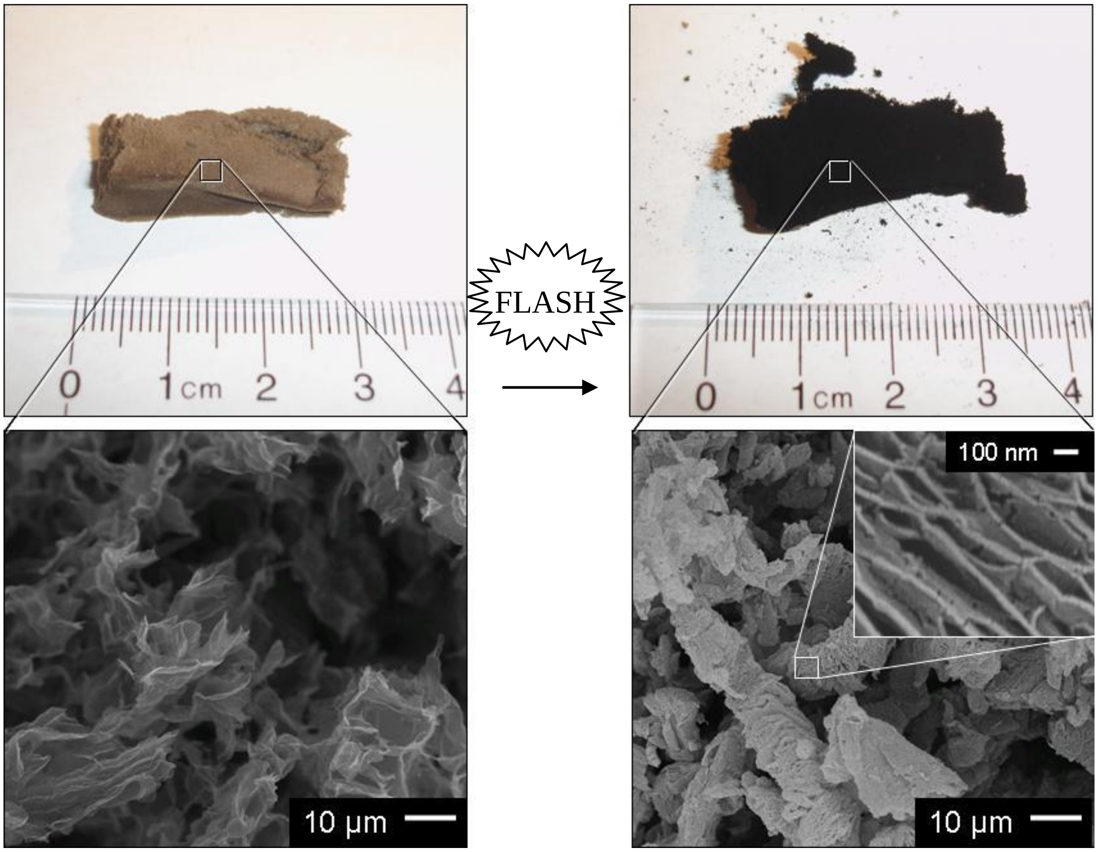

Figure 1 A photo of a light brown GO foam sample (a). A scanning electron micrograph (SEM)of the GO foam shows the porous nature of the foam in greater detail (b). After flashing, the GO foams ignite releasing CO_2 and H_2O as the major products with some CO leaving behind an exfoliated, deoxygenated graphitic carbon (DCG) material as depicted in the photograph (c). An SEM image of the material shows exfoliated layers (d). Under high magnification, (inset (d) the exfoliated layers of carbon measure 10-20 nm in thickness.

When exposing the GO foam samples to the flash, we found the ease of ignition and reaction propagation to be heavily dependant on the density of the GO foam. Denser GO foams (> $50mg/cm^3$) were typically more difficult to ignite requiring several flashes at close range (<1 mm) in order to initiate a reaction. Once ignited however, a reaction front would move through the GO foam structure releasing CO_2 and H_2O as it moved. **Figure 2a** is a photograph of a 15 mg/cm3 GO foam sample undergoing a progressive deflagration reaction to DGC. The image in **Figure 2a** is a still frame taken from a movie as the reaction front moves from left to right after having photothermally ignited the sample on the left end. The light brown area on the right side of the sample is unreacted GO. Analysis of the movie frames indicates the reaction front moves through the material at a rate of 10 cm/sec. The lower density GO foams (< 5 mg/cm^3) although easier to ignite, did not produce enough heat via deflagration to sustain a reaction front, and thus were not self-propagating.

GO foams could be flashed while being contained in an evacuated flask or under inert argon atmosphere by flashing through the transparent glass of the round bottom flask. In both cases the GO foams ignited and the reaction propagated through the bulk of the foam, demonstrating that the deflagration of GO did not require outside oxygen to propagate. **Figure 2b** shows SEM images of GO foams flashed in open atmosphere, and under argon atmosphere **(Figure 2c)**. Unlike the samples flashed under argon, SEM images of the open air flashed samples look as though they contain amorphous carbon at the edges instead of the fine expanded structure found in the argon flashed samples. We attribute this amorphous carbon to secondary burning of the newly formed graphitic carbon in atmospheric oxygen after the removal of H_2O and CO_2 from the primary deflagration reaction.

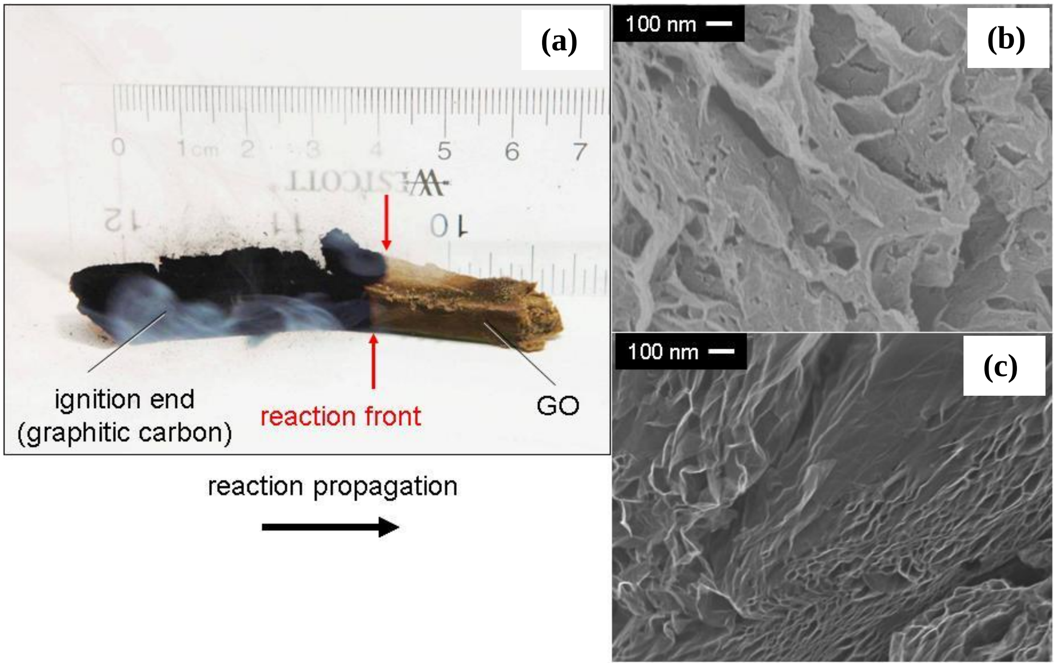

Figure 2 A photo of a 15 mg/ml GO foam sample after photoignition at the left-hand side shows the propagation of the reaction front from left to right. GO foams flashed in open atmosphere typically burn in atmospheric oxygen after deflagration yielding amorphous carbon at the edges as shown in the SEM image (b). If flashed under Ar atmosphere, the GO foams do not burn in atmospheric oxygen after release of CO_2 and H_2O resulting in a more pure exfoliated sample (c).

Characterization of Resulting Graphitic Carbon

The DGC material that remained after photothermally induced deoxygenation was analyzed for carbon and oxygen content using X-ray photoelectron spectroscopy (XPS). The carbon and oxygen content change from 68.7 % and 29.3 % respectively for the GO starting material, to 92.1 % and 7.7 % after flashing. The remaining oxygen is most likely due to residual functionality due to incomplete deoxygenation. **Figure 3a** is an XPS spectrum of GO before flashing and after flashing **Figure 3b**. Upon flashing, the GO foam underwent an average mass loss of 70%. As an interesting side observation, repeated flashing of the expanded DGC material resulted in continued photoacoustic popping sounds and a measurable reduction in mass for each flash exposure. We speculate that the added energy from repeated flashing caused the mostly converted DGC material to continue oxidizing to CO_2. X-ray powder diffraction of a compressed pellet of the DGC shows a broad, low-intensity peak centered at 26.4° 2θ indicating that after deflagration the product is - in fact - graphitic in nature. The peak broadness is most likely due to both the small crystalline domain sizes of the graphitic planes and the turbostatic nature of the expanded sheets. Resistivity measurements of the DGC yield a reduction in resistance from **$9.6 \times 10^5\ \Omega \cdot$ cm (1.0×10^{-3} S/m) for the GO starting material to 2.45 $\Omega \cdot$ cm (40.7 S/m) still *too high(low)*** after reduction. This four order of magnitude resistivity change is consistent with other forms of thermally reduced GO.**[14,15]**

Due to the expanded nature of the flashed GO foams (DGC), they were analyzed for surface area by measuring N_2 uptake using the Braunaur Emmett-Teller (BET) analysis method. Before flashing, a GO foam with a density 15 mg/cm^3 was measured to have a surface area of 6 m^2/g. After flashing, the measured surface area yielded a range from 400 m^2/g to 980 m^2/g. We believe the large range in values can be attributed to difficulties in determining the sample weight and adsorbed water. Hydrogen uptake of the flashed DGC was performed resulting in an uptake of 1.75 % at room temperature. The DGC obtained from flashing GO was found to be dispersible in several aprotic polar organic solvents including: tetrahydrofuran, dimethylformamide, n-methylpyrolidone, and dimethylsulfoxide as is shown in **Figure 3c**.

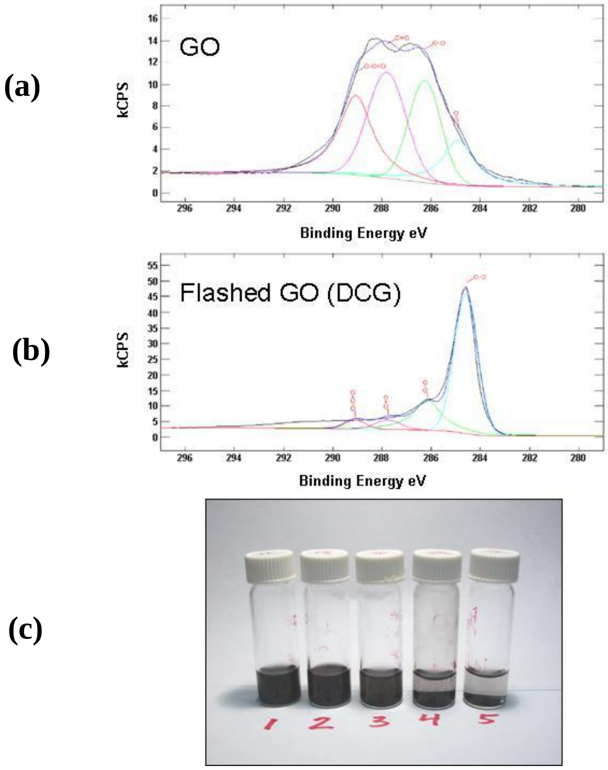

Figure 3 X-ray photo electron spectroscopy (XPS) peak deconvolution of GO (a) yields a C:O ratio of 2.3:1. After flashing the C:O ratio increases to 11.9:1 indicating deoxygenation (b). The residual functionality left behind after incomplete deoxygenation allows the DGC sheets to be dispersed into a variety of polar aprotic organic solvents. DGC obtained after flashing was dispersed into: (1) n-methylpyrolidone (NMP), (2) dimethylfomamide (DMF), (3) tetrahydrofuran (THF), (4) nitromethane, and (5) acetonitrile as shown in the photograph (c)

Patterning Paragraph

In addition to GO foam materials, we attempted to take the idea of photothermal conversion of GO to DGC one step further by flashing GO films. To do this, we created thin GO films (< 1 μm in thickness) by filtering a dilute GO dispersion through a thermally insulating, 0.2 μm nylon Millipore™ filter. **Figure 4a** shows optical microscope images of a copper transmission electron microscope (TEM) grid placed on top of a GO film still attached to the nylon filter. Using the TEM grid as a mask, we flashed the GO film at close range inducing deoxygenation to graphitic carbon. **Figure 4b** is an optical microscope image of the GO film after flashing. Looking at the image, we can see clearly defined regions of black (exposed) and brown (masked) mimicking the TEM grid mask. SEM images of the masked film (**Figure 4c**) show how the exposed regions on the GO film explode outward upon ignition by the flash. This blowing-out of the sheets can most likely be attributed to the release of CO_2 and H_2O.

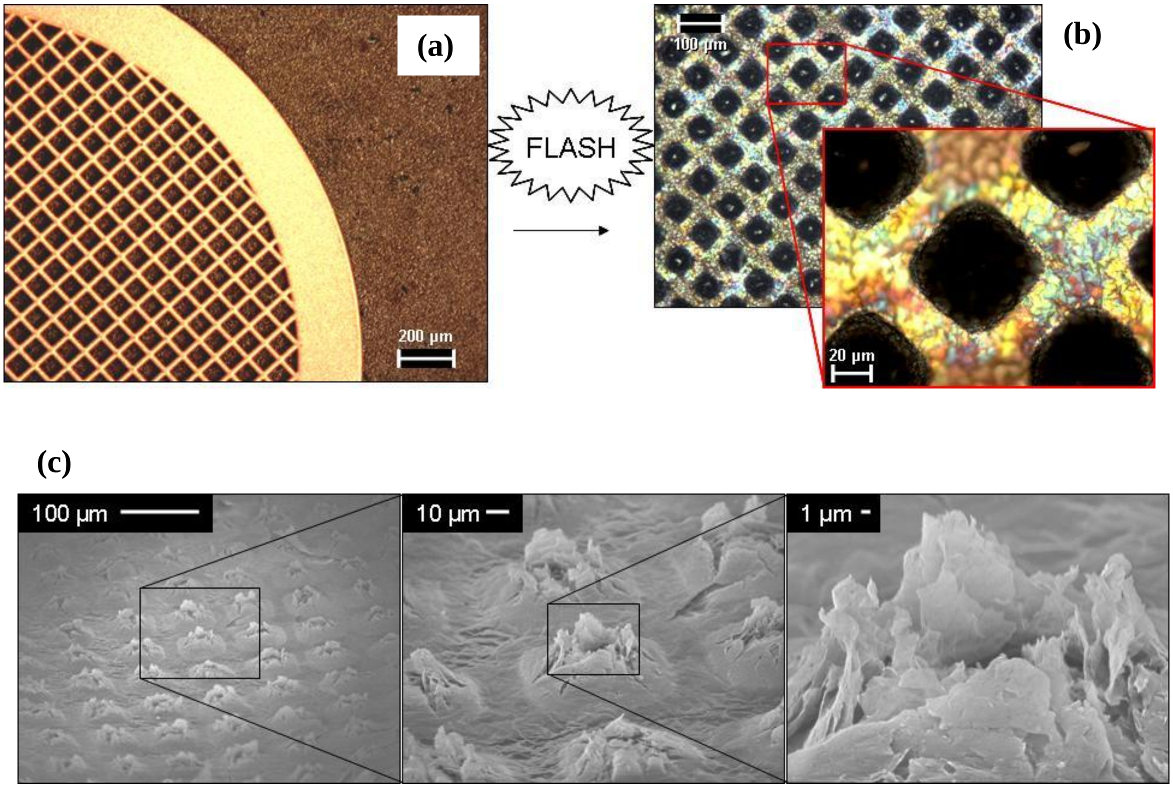

Figure 4 An optical microscope image of a GO film obtained via filtration along with a Cu transmission electron microscopy (TEM) grid before flashing (a). Using the TEM grid as a mask, the pattern of the TEM grid is transferred to the GO film as shown in the optical microscope images (b). The exposed regions turn a dark black in contrast to the masked GO film. The deoxygenation and subsequent release of CO_2 and H_2O blow the platelets of DGC out from the surface as depicted in the series of SEM images (c).

Dist Ignition Paragraph

Apart from patterning applications, one of the more promising applications for photothermally initiated reactions could be as an ignition promoter for fuels. By dispersing GO platelets to a liquid fuel, it would be possible to initiate ignition of the fuel using a flash of light as opposed to a spark plug. Illumination of a fuel/oxidizer mixture would enhance combustion by allowing ignition to occur at numerous locations simultaneously. One of the major drawbacks of an electrical spark is that it is a single-point ignition source. Ideally, multiple ignition nucleation sites allow for more controllable, more efficient and more reliable ignition and combustion. This is of critical importance for applications such as liquid fueled rockets, where current ignition methods are known to possess one or more disadvantages. Issues such as combustion instability and start-up transients not only can cause severe damage, but also degradation in engine efficiency and increase emission of pollutants. It is thought that nearly 30% of the combustion instabilities in rocket engines, leading to engine damages and possible loss of cargo and human life, can be traced back to the nature of the propellant initial energy release process, see Harrje and Reardon.**[39]**

The aforementioned short-comings of the existing systems combined with intuitive engineering advantages of low-energy, lightweight distributed ignition, has motivated some researchers to attempt using single wall carbon nanotubes (SWNTs) as photo-ignition enabling additives to fuels **[32-34]** In these tests, the SWNTs were found to only ignite in the presence of ambient oxygen and did not disperse well in test fuels. Flashing of SWNTs is also heavily dependent on Fe catalyst concentration. Since it carries its own supply of oxygen and is highly dispersible in fuels such as alcohol, GO may show promise as an ignition promoter for fuels. In our preliminary experiments, we have been able to successfully ignite ethanol fuels using GO as a photothermal initiator. **Figure 5a** shows a photo of a sample of GO foam with ethanol vapor being passed over it. After flashing **(Figure 5b)**, the ethanol readily ignited as a result of the GO ignition. After the ethanol fuel is consumed, we can see the DCG glowing bright red as a result of the combustion reaction in **Figure 5c**. Pyrometer readings of this ignition process indicate that by flashing GO we are able to achieve temperatures of 400-500 °C.

Figure 5 A series of photographs shows a sample of GO foam before flash ignition (a). By passing ethanol vapor over the GO foam sample and flashing the GO foam is capable of igniting the ethanol as depicted in the photograph (b). After ignition, the deoxygenated GO sample can be seen glowing red from the energy released during the deflagration reaction (c).

HCCI engine application:

Over the last decade, extraordinary effort has been undertaken to both improve the fuel efficiency in traditional gasoline engines and search for clean, renewable alternatives fuel alternatives to gasoline. One of the ideas that has surfaced from this thrust, is the notion of a homogeneously charge compression ignition (HCCI) engine that combines the high efficiency of a diesel engine with the low emissions of a spark ignition (SI) engine. In a typical HCCI engine, fuel and air are mixed homogeneously similar to a SI engine, but ignition occurs by means of an autoignition under high compression similar to a diesel engine.**[40]** The high compression ratio of HCCI engines provides an efficiency increase of up 15% over current SI engines.**[41,42]** Currently, one of the major challenges facing HCCI engines has been controlling the unpredictable compression-induced ignition process. By using an ignition promoter such as GO, it could be possible to achieve distributed ignition in HCCI engines providing accurate ignition timing resulting in homogeneous detonation of fuel and air.

Summary

Nanoparticles composed of high extinction coefficient materials are able to achieve dramatic temperature increase upon exposure to short pulses of moderate intensity light. These temperature increases occur as a consequence of the increased surface to volume ratio and decreased number of the thermally conducting pathways by which absorbed light energy is lost. One of the distinguishing characteristics that sets photothermal ignition of GO apart from the flashing of other nanomaterials, is that instead of merely igniting or melting a material, we are able to initiate the exothermic decomposition reaction. The benefit of this is that the energy required for ignition is not provided solely by the flash light source as it would be with other nanomaterials. This enables the use of lower power light sources and/or larger particles in order to achieve ignition since the particles themselves add energy to the system. In the future, GO or other oxygen bearing, self decomposing particles like it may make it possible to tune the photoignition behavior of a fuel to provide more controllable distributed ignition. In patterning applications, the solubility differences between GO and DGC can be used to quickly separate exposed and masked regions of a thin GO film. Using an organic solvent the broken-up flashed areas of a GO film could be washed, leaving the masked GO portions intact. Subsequent thermal or chemical reduction of the patterned GO films to conducting, reduced GO would make it possible to create highly conducting patterns.

Acknowledgements:

Hsiao Hu Peng – for freeze dryer
Christina Baker & Henry Tran – Conductivity measurements
Yaghi Lab guy – Hydrogen uptake
Dunn lab guy - BET

References:

1. Ajayan, P. M.; Ramanath, G.; Terrones, M.; Ebbesen, T. W. *Science* **2002**, 297, 192-193.
2. Huang, J.; Kaner, R. B. *Nature Nanotechnology* **2004**, 3, 783-786.
3. Wang, N.' Yao, B. D.; Chan, Y. F.; Zhang, X. Y. *Nano Letters* **2003**, 3, 475-477
4. Ying, J.; Nanostructured Materials. New York: Academic Press, 2001.
5. Brodie, B. *Ann Chim. Phys.* **1855**, 45, 351
6. Dikin, D.; Stankovich, S.; Zimney, E. J.; Piner, R. D.; Dommett, H. B.; Evmenenko, G.; Nguyen, S. T.; Ruoff, R. S. Nature 2007, 448(26), 457-460.
7. Park, S.; Lee, K. S.; Bozoklu, G.; Cai, W.; Nguyen, S.; Ruoff, R. S. *ACS Nano* **2008**, 2(3), 572-578.
8. Stankovich, S.; Dikin, D. A.; Piner, R. D.; Kohlhaas, K. A.; Kleinhammes, A.; Jia, Y.; Wu, Y.; Nguyen, S. T.; Ruoff, R. S. *Carbon* **2007**, 45(7), 1558-1565.
9. Stankovich, S.; Piner, R. D.; Chen, X.; Wu, N.; Nguyen, S. T. Ruoff, R. S.; *J. Mater. Chem.* **2006**, 16, 155-158.
10. Hofmann, U.; Frenzel, A. *Kolloid Z* **1934**, 68, 149-151.
11. Tung, V. C.; Allen, M. J.; Yang, Y.; Kaner, R. B. *Nat. Nano.* **2008**, 4, 25-29.
12. Li, D.; Muller, M. B.; Gilje, S.; Kaner, R. B.; Wallace, G. G. *Nat. Nano.* **2007**, 3, 101-105
13. Park, S.; An, J.; Piner, R. D.; Jung, I.; Yang, D.; Velamakanni, A.; Nguyen, S. T.; Ruoff, R. S. *Chem. Mater.* **2008**, 20(21), 6592-6594.
14. Gilje, S.; Han, S.; Wang, M. S.; Wang, K. L.; Kaner, R. B. *Nano Lett.* **2007**, 7, 3394
15. Gomez-Navarro, C.; Weitz, R. T.; Bittner, A. M.; Scolari, M.; Mews, A.; Burghrd. M.; Kern, K. *Nano Lett.* **2006**, 7, 3499
16. Stankovich, S.; Dikin, D. A.; Dommett, G. H. B.; Kohlhaas, K. M.; Zimney, E. J.; Stach, E. A.; Piner, R. D.; Nguyen, S. T.; Ruoff, R. S. *Nature* **2006**, 442(7100), 282-286.
17. Watcharotone, S.; Dikin, D. A.; Stankovich, S.; Piner, R.; Jung, I.; Dommett, G. H. B.; Evmenenko, G.;Wu, S. E.; Chen, S. F.; Liu, C. P.; Nguyen, S. T.; Ruoff. R. S. *Nano Lett.* **2007**, 7(7), 1888-1892.
18. Chen, H.; Muller, M. B.; Gilmore, K. J.; Wallace, G. G.; Li, D. *Adv. Mater.* **2008**, 999(9), 1-5.
19. Arsat, R.; Breedon, M.; Shafiei, M.; Spizziri, P. G.; Gilje, S.; Kaner, R. B.; Kalantar-zadeh, K.; Wlodarski, W.; *Chem. Phys. Lett.* **2008**, 467(4-6), 344-347.
20. Stoller, M. D.; Park, S.; Zhu, Y.; An, J.; Ruoff, R. S. *Nano Lett.* **2008**,
21. Cote, L. J.; Kim, F.; Huang, J. *JACS* **2009**, 101, 1043.
22. Goki, E.; Lin, Y. Y.; Miller, S.; Chen, C. W.; Su, W. F. Chhowalla, M. *Appl. Phys. Lett.* **2008**, 92, 233305.
23. Wang, X.; Zhi, L.; Tsao, N.; Tomovic, Z.; Li, J.; Mullen, K. *Angew. Chem. Int. Ed.* **2008**, 47, 2990-2992.
24. Wu, J.; Bercerril, H. A.; Bao, Z.; Liu, Z.; Chen, Y.; Peumans, P. *Appl. Phys. Lett.* **2008**, 92, 263302.
25. Goki, E.; Fanchini, G.; Chhowalla, M. *Nat. Nanotechnol.* **2008**, 3, 270-274.

26. Li, X. L.; Zhang, G.; Bai, X.; Sun, X.; Wang, X.; Wang, E.; Dai, H. *Nat. Nanotechnol.* **2008**, 3, 538-542.
27. Schneipp, H. C.; Li, J. L.; McAllister, M. J.; Sai, H.; Herrera-Alonso, M.; Adamson, D. H.; Prud'homme, R. K.; Car, R.; Saville, D. A.; Aksay, I. A. *J. Phys. Chem. B.* **2006**, 110, 8535-8539.
28. Li, J. L.; Kudin, K. N.; McAllister, M. J.; Prud'homme, R. K.; Aksay, I. A.; Car, R.; *Phys. Rev. Lett.* **2006**, 96, 176101.
29. Ramanathan, T.; Abdala, A. A.;Stankovich, S.; Dikin, D. A.;Herrera-Alonso, M.; Piner, R. D.; Adamson, D. H.; Schniepp, H. C.; Chen, X.; Ruoff, R. S.; Nguyen, S. T.; Aksay, I. A.; Prud'homme, R. K.; Brinson, L. C.; *Nat. Nanotechnol.* **2008**, 3(6), 327-331.
30. Boehm, H. P.; Scholz, W. *Zeitschrift fur anorganische und allegemeine Chemie* **1965**, 335, 74-79.
31. Zuckerman, J. J.; Hagen, A. P.;*Oligomerization and Polymerization Formation of Intercalation Compounds, Volume 17, Inorganic Reactions and Methods.* New York, VCH Publishers Inc.1990.
32. Chehroudi, B.; Danczyk, S. A. Global Powertrain Congress World Powertrain Exposition. Novi Michigan. September 2006.
33. Sciamanna, S.; Munson, C.; Dieckmann, G.; US Patent Appl #11/613,105
34. Beiver, C. *New Scientist Magazine* **2005**, 2526,30
35. Braidy, N.; Botton, G. A.; Adronov, A.; Nano Lett. **2002**, 2, 1277.
36. Smits, J.; Wincheski, B.; Namkung, M.; Crooks, R.; Louise, R.; *Mater. Sci. Eng. A* **2003**, 358, 384-389.
37. Chiang, I. W.; Brinson, B. E.; Huang, A. Y.; Willis, P. A.; Bronikowski, M. J.; Margrave, J. L.; Smalley, R. E.; Hauge, R. H. *J. Phys. Chem. B.* **2001**, 105(35), 8297-8301.
38. Chen, H.; Diebold, G.; *Science* **1995**, 270, 963
39. Harrje, D. T.; Reardon, F. H.; Liquid propellant rocket combustion instability, NASA SP-194, *Scientific and Technical Information Office*, Washington, D.C. **1972**.
40. Chehroudi, B. Homogeneous charge compression ignition (HCCI) engine, *Powertrain Iinternational* **2002**, 5(1), 6-10.
41. Magnus, S.; Dec, J. E.; Cernansky, N. P. *Society of Automotive Engineers*. **2005**, 1, 0113.
42. Fukwon, Z.; Asmus, T. W.; Assanis, D. N.; Dec, J. E.; Eng, J. A.; Najt, P. M. *Society of Automotive Engineers* **2**

Supplementary Info

Synthesis:

Graphene oxide was synthesized using a modified Hummer's method reported previously. **[14]** Dispersions of GO were freeze-dried in a **(insert freeze-dryer system)**. Dispersion concentrations of 30 mg/ml, 15 mg/ml, 7.5 mg/ml and 3.25 mg/ml were freeze-dried resulting in porous GO materials with densities of 0.03 g/cm^3, 0.015 g/cm^3 and 0.0075 g/cm^3 and 0.00325 g/cm^3 respectively. Film samples of GO were obtained by filtration of a GO dispersion through a 0.22 μm Anapore™ filter for free standing films, and a 0.2 μm Nylon Millipore™ filter for thin films that remained bound to the filter membrane for stability.

Analysis:

X-ray diffraction (XRD) is carried out using a PANalytical XPert Pro diffractometer with Cu Kα radiation ($\lambda = 1.5418$ Å). Before taking X-ray scans the GO is dried for 48 h under vacuum at room temperature followed by 24 h under vacuum over P_2O_5 which acts as a drying agent.[1] Powder X-ray diffraction can be used to verify that the oxidation reaction has reached completion since the introduction of oxygen moieties expands the interplanar galleries in graphite from 3.34 Å to ~6.9 Å.[1,3, 4] Our graphite oxide exhibits a characteristic peak at 12.75 degrees 2θ corresponding to the 002 interplanar spacing of 6.94 Å, while the most intense peak from the starting graphite at 26.4 degrees 2θ, corresponding to a d-spacing of 3.34 Å, is completely absent. The d-spacing of slightly >6.9 Å for the synthesized GO indicates that despite drying under vacuum for 24 h, some water has been absorbed by the GO.

Thermogravimetric analysis (TGA) is carried out using a Perkin Elmer Pyris Diamond TG/DTA. For TGA, the temperature was ramped from 25 – 800 °C at a rate of 5 °C/min under dry air. TGA data is consistent with the formation of graphite oxide (GO) containing some residual water. A TGA indicates weight loss at ~200 °C and ~450 °C corresponding to the loss of water and decomposition of GO, respectively.[5] The GO is completely decomposed by the time the temperature reaches 600 °C.

The GO and DGC samples were inserted into the analysis chamber of a ThermoVG ESCALAB 250, X-ray photoelectron spectrometer. Spectra were obtained by irradiating the sample with a 320 μm diameter spot of monochromated aluminum Kα X-rays at 1486.6 electron Volts (eV) under ultrahigh vacuum conditions. The analysis consisted of acquiring 10-20 scans and signal averaging. The survey scans were acquired with a pass energy of 80 eV, and the high resolution scans were acquired with a pass energy of 20 eV. Low pressure gas adsorption isotherms were measured volumetrically on an Autosorb-1 analyzer (Quantachrome Instruments).

A liquid nitrogen bath (77 K) was used for N_2 and H_2 isotherm measurements. The N_2, H_2, and He gases used were UHP grade. For measurement of the apparent surface areas (SLang), the Langmuir method was applied using the adsorption branches of the N2 isotherms assuming a N2 cross-sectional area of 16.2 A2/ molecule. The micropore volumes (Vp) were determined using the Dubinin-Raduskavich (DR) transformed N2 isotherms across the linear region of the low pressure data.

Conductivity data was obtained using a Jandel RM3-AR resistivity tester using an applied current of 4.532 μA. Optical microscope images were taken using a Zeiss AxioTech 100 reflected light microscope with Zeiss AxioCam MRc camera. UV-vis spectra were acquired on a Shimadzu UV-3101PC, software used is Shimadzu UVProbe version 2.21. The absorbance wavelength spectrum was scanned is from 190 through 800nm.

Flash Characterization:

The films were flashed using a Pro Master FA1000 being fired in "test" mode. The pulse duration of the camera flash was on the order of milliseconds. The integrated pulse energy and duration of the flash was measured using a Molectron Opti-mum4001, 4-channel joulemeter in combination with a model J25 detector.

A UV-vis spectrum of GO reveals a broad peak in absorbance with a maximum centered around 230 nm trailing off at higher wavelength. Since most commercially available camera flashes utilize a UV filter to more accurately simulate the color temperature of sunlight, we found that removal of the polycarbonate UV filter allowed us to flash the GO foam samples from further away or through thick glass. When flashing GO samples through glass, the glass tends to act as a thermal barrier sheilding the samples from the heat developed by the Xe discharge tube. Since only the light from the flash is allowed through, we believe the photo-ignition of GO to occur strictly as a result of absorbed light energy being converted into heat by the GO, with no contribution from the heat of the Xe flash tube. The flash energy typically increased as the charging capacitor in the photographic flash unit was allowed to charge for longer periods of time. By firing the flash immediately after the "test flash" button illuminated, greater repeatability could be achieved. Five measurements were taken at each distance with a standard deviation less than 4%. Typical flash durations ranged from 1-2 milliseconds. . **Figure S1** shows a plot of the total integrated fluence (J/cm^2) released by the flash in as a function of distance from the flash. The two lines in **Figure S1** correspond to the flash energy with and without the UV filter in place. The maximum ignition distance for a 15 mg/ml GO foam with and without the UV filter in place was measured and is indicated in **Figure S1**. We found that although the total energy increased only slightly at each distance by removing the UV filter, ignition of the GO foam could be achieved at further distances – and there for lower total energy – than when the UV filter was in place. The GO foams typically ignited at a distance of ~1mm with the UV filter in place corresponding to a fluence of 250-300 mJ/cm^2. After removing the UV filter, the same GO foam could be ignited at a distance of 13-15 mm corresponding to < 200 mJ/cm^2. We speculate that since GO absorbs more heavily in the UV, more energy was being absorbed and there for converted into heat after removal of the UV filter allowing ignition at lower total energy levels.

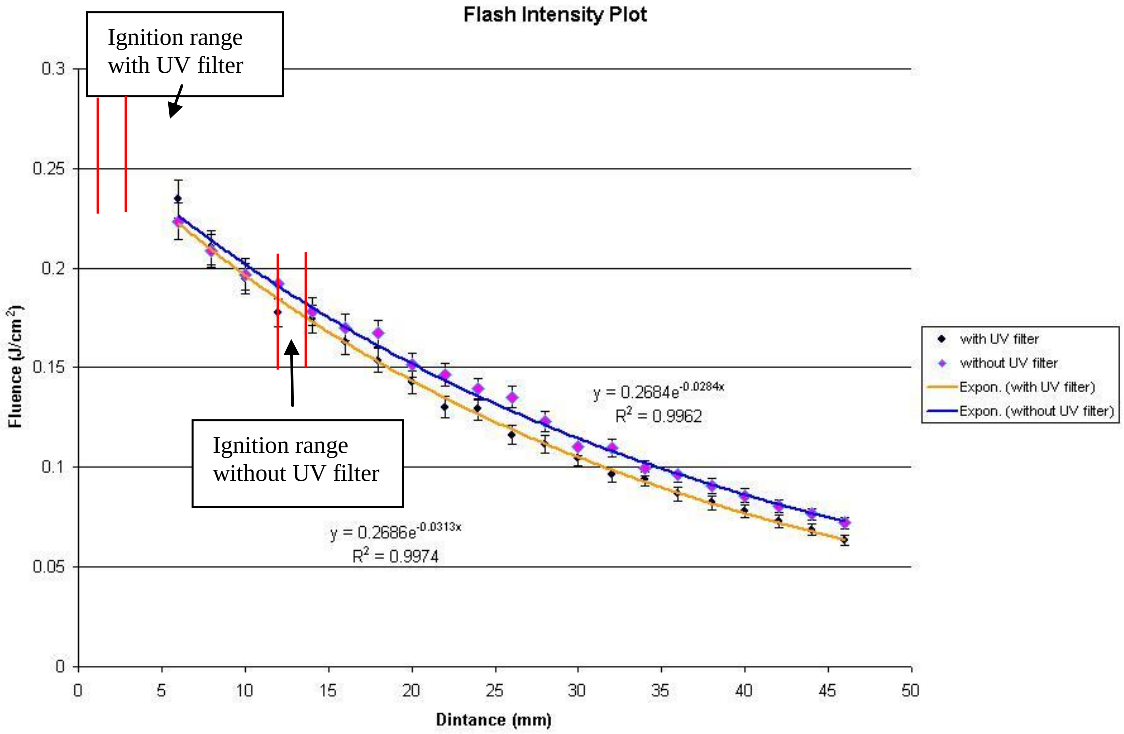

Figure S1 Using a pulse energy meter the total integrated energy of the camera flash was plotted as a function of distance from the flash with and without the UV filter built into the flash. The energy was normalized per unit area to give the fluence (J/cm^2) of the flash at a given distance. Even though the total energy of the flash increased only marginally without the UV filter as opposed to the flash with the filter, the energy required to ignite the GO foam was considerable less without the UV filter. Since GO absorbs more heavily in the UV (ε_{max} = 231 nm) it is no surprise that by removing the UV filter from the flash, ignition of GO at lower energies can be achieved.